ELSEVIER

Full paper / Mémoire

Estimating the stabilities of actinide aqueous species. Influence of sulfoxy-anions on uranium(IV) geochemistry and discussion of Pa(V) first hydrolysis[☆]

Pierre Vitorge [a,b,*], Vannapha Phrommavanh [c], Bertrand Siboulet [d], Dominique You [a], Thomas Vercouter [a], Michael Descostes [b,c], Colin J. Marsden [e], Catherine Beaucaire [c], Jean-Paul Gaudet [f]

[a] *Laboratoire de spéciation des radionucléides et des molécules (LSRM), CEA Saclay, DEN/DANS/DPC/SECR, 91191 Gif-sur-Yvette cedex, France*
[b] *UMR 8587, CEA Saclay, DEN/DANS/DPC/SECR, 91191 Gif-sur-Yvette cedex, France*
[c] *Laboratoire de mesures et modélisation de la migration des radionucléides (L3MR), CEA Saclay, DEN/DANS/DPC/SECR, 91191 Gif-sur-Yvette cedex, France*
[d] *CEA Marcoule, DEN/DRCP/SCPS, 30207 Bagnols-sur-Cèze cedex, France*
[e] *Laboratoire de physique quantique, CNRS−UMR 5626, Université Paul-Sabatier, 118, route de Narbonne, 31062 Toulouse cedex 4, France*
[f] *Laboratoire d'étude des transferts en hydrologie et environnement (LTHE), UMR 5564, CNRS/INPG/IRD/UJF, BP 53, 38041 Grenoble cedex 9, France*

Abstract

Qualitative chemical information is used as a guideline for correlations between equilibrium constants or between equilibrium constants and atomic charges (deduced from quantum mechanics calculations). Pa(V) and Nb(V) hydrolysis constants are also recalculated from experimental data. $\log K_1^\circ(\mathrm{An^{IV}/RO_2^{2-}}) = 6.5_9 \pm 0.5_5$ $(\mathrm{S_2O_3^{2-}})$, $10.0_6 \pm 0.8_8$ $(\mathrm{SO_3^{2-}})$, $11.9_7 \pm 1.0_7$ $(\mathrm{CO_3^{2-}})$, and $10.0_5 \pm 0.8_8$ $(\mathrm{HPO_4^{2-}})$ are estimated based on the trend of affinity for An cations in the series $\mathrm{CO_3^{2-}} > \mathrm{HPO_4^{2-}} \approx \mathrm{SO_3^{2-}} > \mathrm{SO_4^{2-}} \approx \mathrm{S_2O_3^{2-}}$. These ideas and values are used to discuss U(IV) chemistry in S-containing ground-waters. *To cite this article: P. Vitorge et al., C. R. Chimie 10 (2007).*
© 2007 Académie des sciences. Published by Elsevier Masson SAS. All rights reserved.

Résumé

Des connaissances qualitatives ont été concrétisées sous la forme de corrélations empiriques entre constantes d'équilibres, voire avec les charges atomiques (issues de calculs quantiques) dans la série $\mathrm{CO_3^{2-}} > \mathrm{HPO_4^{2-}} \approx \mathrm{SO_3^{2-}} > \mathrm{SO_4^{2-}} \approx \mathrm{S_2O_3^{2-}}$, pour, par exemple, estimer $\log K_1^\circ(\mathrm{An^{IV}/RO_2^{2-}}) = 6.5_9 \pm 0.5_5$ $(\mathrm{S_2O_3^{2-}})$, $10.0_6 \pm 0.8_8$ $(\mathrm{SO_3^{2-}})$, $11.9_7 \pm 1.0_7$ $(\mathrm{CO_3^{2-}})$, et $10.0_5 \pm 0.8_8$ $(\mathrm{HPO_4^{2-}})$.

1. Introduction

The geochemical behaviour of actinides have been extensively studied for understanding uranium and thorium ore deposits, and more recently for assessing the environmental impact of the possible disposal of wastes that contain Pa, Np, Pu, Am or Cm. Starting with uranium [1], the Thermochemical Data Base project of the Nuclear Energy Agency (NEA-TDB) organised the reviewing of published experimental data relevant for modelling aqueous chemistries and solubilities of the most important radionuclides. The results of the NEA-TDB project are now well accepted as a reference critical review, essentially for aqueous chemistry and solubility at room temperature, but these reviews proposed data only when convincing experimental validations were published. There is therefore a gap between this restricted set of quantitative validated thermochemical data and qualitative chemical knowledge.

However, besides selected numerical values, the NEA-TDB reviews also provide qualitative information [2,3], which we used together with analogies for estimating the hydrolysis constants and standard potentials [4] needed for drawing Pourbaix' diagrams of actinides [5]. The present paper aims at testing such rough estimates for complexation.

Rules of thumb are currently used by chemists for checking the possible formation of hypothetical chemical species in specific chemical conditions, when these chemical species are not in databases. This might typically be the case for the environmental aqueous chemistry of An(IV), the actinide elements at the +4 oxidation state (An = Th, U, Np and Pu) in the presence of S-containing inorganic ligands; for this reason it is also an aim of the present paper to estimate the stabilities of An(IV) complexes with sulfoxy-anions.

For storing radioactive wastes, several projects are looking for geological sites that are well isolated from surface waters. These often correspond to anoxic conditions, where U, Np and Pu are expected to be stable in the +4 oxidation state [2,4]. Interestingly, chemical analogues are Ce(IV) and Th, and probably Zr and Hf.

Selected NEA-TDB equilibrium constants and redox potentials [2] are adequate for reliable modelling of uranium chemistry in most equilibrated groundwaters. Uranium is predicted to be stable in anoxic waters in the form of the $U(OH)_4(aq)$ aqueous species in equilibrium with uraninite, $UO_2(s)$, a compound of low solubility [2,5,6]. Similar behaviour is expected for Np and Pu, even though Pu^{3+} might also be stable [4–7].

In natural under-ground-waters CO_3^{2-}, the carbonate anion is often the dominating ligand among the inorganic ligands (for actinide cations). However, carbonate complexes are predicted to be of little important for An(IV) [2,4,7]. Nevertheless, many $An(CO_3)_i(OH)_j^{4-2i-j}$ complexes have been proposed, but no reliable values could be validated for most of the corresponding formation constants [2,4], for which maximum possible values have been estimated from experimental observations, that also confirmed the similar behaviour of Th, U(IV), Np(IV) and Pu(IV) in carbonate/bicarbonate aqueous solutions [4,5,8]. Values have recently been proposed for the formation constants of several $Th(CO_3)_i(OH)_j^{4-2i-j}$ complexes in an attempt to interpret a solubility study of $ThO_2(s)$ [8,9], but the $Th(CO_3)_4^{4-}$ species were not included in the interpretation, even though we shall see it should not be completely negligible according to the NEA-TDB data [4]. For probing such competition between the HO^- and CO_3^{2-} ligands, the relative stabilities of the corresponding 1:1 complexes of An^{4+} will be compared. In this framework, the stability of $AnCO_3^{2+}$ will be estimated: its existence has never been demonstrated, since it is always hidden by hydrolysed species. This over-stabilisation of hydrolysis is specific to the +4 oxidation state: the 1:1 carbonate complexes are well known, and their stabilities were well established for An(III), An(V) and An(VI) (it is not known for Pa(V), which is known to have a very different aqueous chemical behaviour from the other An(V)).

Several other inorganic hard anions are quite reactive toward actinide cations, specially those of high charge (PO_4^{3-}), of small size (F^-), or polydentate (HPO_4^{2-}): depending on their content in groundwaters they might form complexes with actinide cations. For example, it

was recently proposed that the pore-waters of Callovo–Oxfordian clay minerals, where an underground research laboratory is being built to study the feasibility of a deep geological repository for radioactive wastes in France [10], contain quite large amounts of SO_4^{2-}. The pore-water composition is approximately at the $SO_4^{2-}/HS^-/H_2S$ frontier point (Fig. 1). Although the most stable aqueous sulfur species - those bolded on Pourbaix' diagrams - are sulfide (HS^-) and sulfate (SO_4^{2-}), some other sulfoxy-anions are often detected in natural environments, typically as thiosulfate ($S_2O_3^{2-}$) and sulfite (SO_3^{2-}) ions. For example, about 25% of the total S content has been reported to be $S_2O_3^{2-}$ in a reducing groundwater [11], and even in more oxidizing conditions [12]. Sulfoxy-anions are also suspected to form in the course of the oxidative dissolution of pyrite (FeS_2) [13], a mineral often associated with the redox regulation of ground-waters. For this reason, we focus on sulfoxy-anion ligands, specially on $S_2O_3^{2-}$.

Grenthe et al. have selected complexing constants for U(VI) complexes with these anions [2], but they wrote in their review that confirmation is needed: "*The only quantitative information about aqueous uranium thiosulfate complexes is the study by Melton and Amis […] This review tentatively accepts [their] value, (although confirmation of the results from another study would be useful)*". Furthermore: "*The solid formed seems to be a mixture indicating decomposition of thiosulfate into sulfite and elemental sulfur. This review finds no reliable evidence for the formation of solid uranium thiosulfate compounds.*" This decomposition might very well be the result of redox reactions (disproportionation), since both uranium and sulfur have a wide range of possible oxidation states, and their stability domains are not well established in mixtures of uranium and sulfur. This might in fact be a problem for other uranium compounds and complexes with sulfur-containing ligands. Unfortunately the NEA-TDB reviews could not validate such data for the Th and Zr analogues [14,15]. Since the NEA-TDB review has selected data for a thiosulfate complex of U(VI) [2], one might very well expect thiosulfate complexes of U(IV) in more reducing conditions — unless thiosulfate is strongly reduced, when U(IV) is formed — because the U^{4+} hard cation is usually more reactive (than UO_2^{2+}) toward oxygen-donor ligands. Based on the same hardness rule, thiosulfate should bind to hard cations *via* the O rather than the S atom of the sulfoxy-anion ligands. The same problem holds for the U/SO_3^{2-} system: the NEA-TDB review has selected data for sulfite complexes of U(VI); but not for U(IV): "*Formation of*
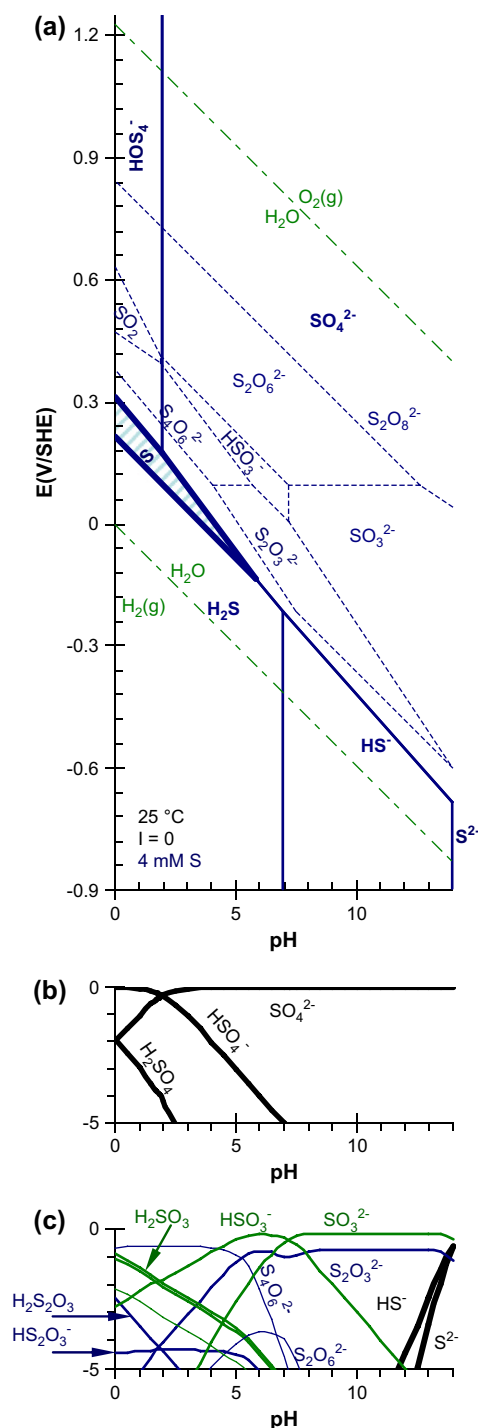
Fig. 1. Pourbaix diagram of sulfur. (a) The names of the major species (HS^-, H_2S, SO_4^{2-}, HSO_4^- and solid S) are in bold, and their predominance domains are drawn with thick lines. The domains (thin dashed lines) of the other (minor sulfur) species are obtained by suppressing SO_4^{2-}, HSO_4^- and H_2SO_4. (b and c) The speciation (namely $\log[H_iS_jO_k^z]/[S]_{total}$) of each species ($H_iS_jO_k^z$) is represented for two kinetic assumptions (see text) in redox conditions corresponding to line B of Fig. 6.

aqueous uranium(IV) sulfite complexes was reported in a qualitative study by Rosenheim and Kelmy. However, no experimental chemical thermodynamic data on these species are available." As a probe for ligand competition (between $S_2O_3^{2-}$ or SO_3^{2-} and typically OH^- or CO_3^{2-}), we shall estimate the formation constants of the corresponding 1:1 An(IV) complexes, namely $AnS_2O_3^{2+}$ and $AnSO_3^{2+}$.

Various methods are commonly used for estimating equilibrium constants, typically as empirical correlations with physical (or phenomenological) parameters (atomic radii and charges, solvent interactions…). They can also be obtained from molecular modelling methods. Indeed we recently estimated an uncertainty of 10 kJ mol^{-1} on $\Delta_r G$ for Pa(V) hydrolysis [16], which is about 20 times higher than the uncertainty of the experimental determinations of equilibrium constants and standard redox potentials in aqueous solutions. Furthermore, such methods need caution, when using calculated energies [17]. After others [18,19] (with a comment in Ref. [7]) we also tested empirical correlations, which appear to work surprisingly well for some of them: they actually help in putting numbers for quite encyclopedic qualitative knowledge. It is also a way to check such knowledge and corresponding chemical intuition. We use such correlations here, hoping this special issue will help such rules of thumb used by actinide chemistry specialists to become less mysterious. The rough estimates are only guidelines, which need experimental confirmation. They often originate in geometrical and electrostatics reasoning. Indeed, the chemical stabilities of hard cations are often correlated with the charge^2/radius ratios of the reactants. Nevertheless, we shall see that the best correlations are not specially with the atomic charges; correlations between measured equilibrium constants will often appear to fit better: several physical contributions probably cancel out in those cases.

The present paper is organised as follows. First, definitions are given, together with features and explanations of methodologies from the NEA-TDB reviews. Results are first reported for correlations between U(VI) (or analogous An(VI)) 1:1 (1 cation with 1 ligand) complexes and protonation of the corresponding ligands, two types of reactions for which many published data are available. In a next step, such correlations are extended to An(III) and An(V). There are virtually no reliable published 1:1 complexing constants of An(IV), since An^{4+} hydrolysis usually overcomes complexation. Consequently we shall estimate An(IV) 1:1 complexing constants. We shall also consider the position of Pa(V) in our correlations, since its chemical behaviour is an exception as compared to that of the other An(V): this

comparison will be based only on hydrolysis data, since there are very few other published equilibrium constants for Pa(V) aqueous complexes. Prior to this comparison, we shall examine the impact of our estimated complexing constants on the geochemical behaviour of U(IV).

2. Methods

2.1. Equilibrium constants

For consistency, we used reaction data − i.e. $\Delta_r G^\circ$ (equivalently standard equilibrium constants and potentials of redox couples) − they were preferred to formation data ($\Delta_f G^\circ$) [2].

$$K_1^\circ = \frac{|ML^{z_M+z_L}|}{|M^{z_M}||L^{z_L}|} \tag{1}$$

where $|A|$ is the activity of species A.

$$K_a^\circ = \frac{|H^+||L^{z_L}|}{|HL^{1+z_L}|} \tag{2}$$

$pK_a^\circ = -\log K_a^\circ$ is $pH_{1/2}$, the pH at the half-point reaction (where $|L^{z_L}| = |HL^{1+z_L}|$). pK_a° appears to be the ionic product of water, when $L^{z_L} = OH^-$ and when using $|H_2O| = 1$; but when comparing the complexing strengths of various ligands we used the concentration of liquid water: $|H_2O| = C_{H_2O}$ (55.34 mol kg^{-1}). Superscript $^\circ$ stands for infinite dilution (ionic strength, $I = 0$), the standard conditions (see Section 2.2).

$\log K_1^\circ$ values were plotted as a function of pK_a°, for example when K_1° is the formation constant of $AmCO_3^{2+}$, $1/K_a^\circ$ is the protonation constant of CO_3^{2-}. We observed

$$\log K_{1,x}^\circ = a_x + b_x pK_a^\circ \tag{3}$$

linear correlations, where we fitted the a_x and b_x parameters for a series of actinides (or analogues) of the same oxidation number X: $An(X) = M^{z_M} = An^{3+}$, An^{4+}, AnO_2^+ or AnO_2^{2+}. $10^a = K_1^\circ(K_a^\circ)^b = |ML^{z_M+z_L}||H^+|^b/(|M^{z_M}||L^{z_L}|^{1-b}|HL^{1+z_L}|^b)$ is obtained from Eqs. (1)−(3): it is actually an equilibrium constant. When $b = 1$, it simplifies into the $10^{a(1)} = K_1^\circ K_a^\circ = |ML^{z_M+z_L}||H^+|/(|M^{z_M}||HL^{1+z_L}|)$, the

$$M^{z_M} + HL^{1+z_L} \rightleftharpoons ML^{z_M+z_L} + H^+ \tag{4}$$
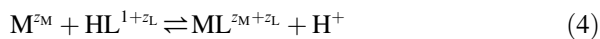
exchange equilibrium constant: $|L^{z_L}|$ cancels out in $K_1^\circ K_a^\circ$ ($= 10^{a(1)}$), which is now the same for all the reactions; it also only depends on a, not on each K_a° (or equivalently K_1°). In that case, the half-point reaction definition is $[|H^+|/|M^{z_M}|]_{1/2} = K_1^\circ K_a^\circ$: a solution of

activity $|H^+|$ has the same reactivity (for the L^{z_L} ligand) as a solution of activity $|M^{z_M}|10^{a(1)}$. Conversely, when the (b) slope is not 1, this simple equivalent solution definition is no longer relevant: the general half-point reaction definition is $10^a = K_1^\circ(K_a^\circ)^b = [(|H^+||L^{z_L}|)^b/(|M^{z_M}||L^{z_L}|)]_{1/2}$, whose interpretation is less intuitive. Furthermore the constant of the exchange equilibrium (Eq. (4)) is now specific for each reaction: $K_1^\circ K_a^\circ = 10^a(K_a^\circ)^{1-b} = 10^{a/b}(K_1^\circ)^{1-1/b}$ depends on each K_a° (or equivalently K_1°), not only on a and b.

Since b_x did not seem to strongly depend on X, we finally used the same b_x (=b) value for all the oxidation states; in that case, for comparing An(X) complexes with An(VI) ones, we used:

$$10^{a_X - a_{VI}} = \frac{K_{1,X}^\circ}{K_{1,VI}^\circ} = K_{X/VI}^\circ = \frac{|ML^{z_M+z_L}||AnO_2^{2+}|}{|AnO_2L^{2+z_L}||M^{z_M}|} \quad (5)$$

the constant of the

$$AnO_2L^{2+z_L} + M^{z_M} \rightleftharpoons ML^{z_M+z_L} + AnO_2^{2+} \quad (6)$$
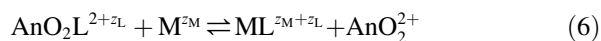
exchange equilibrium. This AnO_2^{2+}/M^{z_M} exchange equilibrium is similar to the H^+/M^{z_M} one (Eq. (4)), where now the half-point reaction definition is $[|AnO_2^{2+}|/|M^{z_M}|]_{1/2} = K_{x/VI}^\circ$: a solution of activity $|AnO_2^{2+}|$ has the same reactivity (for the L^{z_L} ligand) as a solution of activity $|M^{z_M}|K_{x/VI}^\circ$. Similarly, for comparing hydrolysis equilibria, we used the

$$AnO_2OH^+ + M^{z_M} \rightleftharpoons MOH^{z_M-1} + AnO_2^{2+} \quad (7)$$
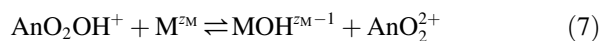
hydrolysis competition equilibrium of constant

$$\frac{{}^*K_{1,x}^\circ}{{}^*K_{1,VI}^\circ} = {}^*K_{X/VI}^\circ = \frac{|MOH^{z_M-1}||AnO_2^{2+}|}{|AnO_2OH^+||M^{z_M}|} \quad (8)$$

where

$$ {}^*K_{i,X}^\circ = \frac{|M(OH)_i^{z_M-i}||H^+|}{|M(OH)_{i-1}^{z_M-i+1}|} \quad (9)$$

is a classical stepwise standard equilibrium constant. $-\log {}^*K_{i,x}^\circ$ is $pH_{1/2}$.

2.2. Activity coefficients

For ionic strength corrections, we used γ_i, the molal activity coefficient of ion i calculated with the "Specific Interaction Theory", the SIT formula [2,4]. The corresponding ε_{ij} empirical (pair interaction) coefficients are taken from the NEA-TDB reviews [4]:

$$\log \gamma_i = -z_i^2 D + \sum_j \varepsilon_{ij} m_j \quad (10)$$

In most cases, the summation could here be restricted to the ClO_4^- and Na^+ (dominating) counter-ions ($= j$). m_j is j (molal) concentration (mol per kg of pure water). Molar ($M = mol\,L^{-1}$) to molal conversion coefficients are tabulated in Handbooks (including the cited NEA-TDB books):

$$D = \frac{A\sqrt{I_m}}{1 + B_r\sqrt{I_m}} \quad (11)$$

is a Debye−Hückel term, where I_m is molal I, $A = 0.509[298\varepsilon_{298}/T\varepsilon_{r,T}]^{1.5}[d_{298}/d_T]^{0.5}$ $kg^{1/2}$ $mol^{-1/2}$, and $B = 3.28 \times 10^9$ $[298\varepsilon_{298}d_T/(T\varepsilon_{r,T}d_{298})]^{0.5}$ $kg^{1/2}$ $mol^{-1/2}$ m^{-1} are calculated from physical constants, and $\varepsilon_{r,T}$ the relative dielectric constant of the solvent (water) and d_T the density at absolute temperature T. r accounts for geometric exclusion about ion i. r is assumed to be constant, $B\,r = 1.5\,kg^{1/2}\,mol^{-1/2}$ at 25 °C, an approximation that enables many measured mean activity coefficients of strong inorganic aqueous electrolytes to be fitted [2]; it corresponds to $r = 4.57 \times 10^{-10}$ m, which appears to be of the correct order of magnitude for most inorganic hydrated ions including their first hydration sphere (by definition if a counterion stays in the first hydration sphere, it is treated as complex formation, not non-ideality). Furthermore, $B\sqrt{I} = 1/l_D$, where l_D is the Debye distance, the distance between an ion and its counter-ion atmosphere: 3.05×10^{-10} m (at 25 °C and $I = 1$ M) in the SIT approximation. The Debye−Hückel formula is valid for large l_D namely for $l_D >> r$: $B\,r = 1.5\,kg^{1/2}\,mol^{-1/2}$ corresponds to $r/l_D = 1.5\sqrt{I_m} << 1$. Indeed the Debye−Hückel formula (D term alone) is only valid at ionic strengths less than 10 or 1 mM, while the SIT formula is usually a good approximation for aqueous solutions with ionic strength up to 4 mol kg^{-1} [2]. The use of ε_{ij} empirical coefficients certainly partly compensates systematic errors (of D in the SIT formula), which might very well explain why the numerical values for ε_{ij} are correlated with the size and the charges of the ions (Fig. 2).

Unknown ε_{ij} numerical values can be estimated by analogy with ions of same charge and similar sizes [3,4]. In that case it was proposed to increase the ε_{ij} uncertainties by ±0.05 kg mol^{-1} [4]. Moreover, we observed a reasonable linear correlation between interaction coefficients and the charge/radius ratios (Fig. 2(a)). For this correlation we used the formal charge of the cation (or the complex), which is indeed the charge seen by the (ClO_4^-) counter-anion at large distance. Unfortunately this assumption does not hold for high ionic strengths, the only conditions where the ε_{ij} m_j term cannot be neglected. Indeed some data for
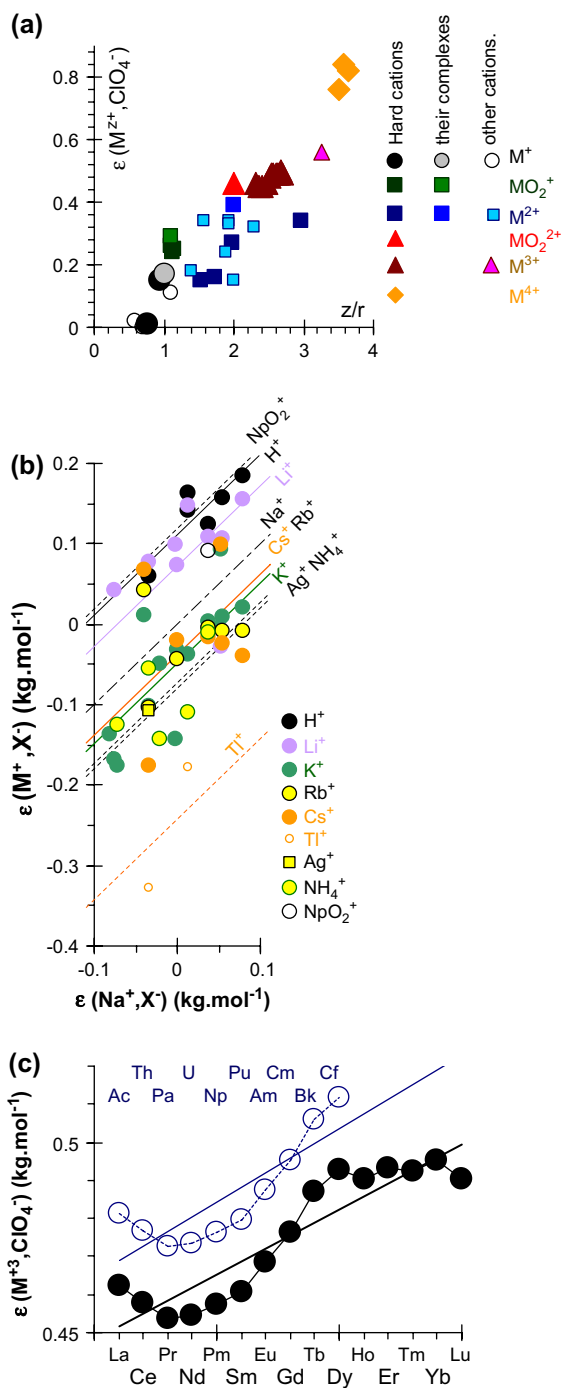
Fig. 2. Empirical correlations for estimating SIT ion pair coefficients.

figure), when using the atomic charge (Section 2.3) of An (in AnO_2^{X-4}, for this reason, we also plotted other correlations without using the charges (Fig. 2(b) and (c))).

2.3. Quantum calculations

In our hydrolysis correlation study, we used the formal charges of An^{3+} (3) and An^{4+} (4), while we used the atomic charge of An(X) in AnO_2^{X-4} ($X = 5$ or 6). This latter was deduced from quantum (DFT) calculations performed at the same calculation levels (ECP and basis sets) as in our recent previous works [17,20], from which we extracted NPA atomic charges [21,22]. Note that in Gaussian98 and 03, these NPA charges are calculated with the NBO software, which is known to consider the UO_2^{2+} 6d orbitals as Rydberg orbitals, despite the final result gives the 7s5f6d electronic configuration. This overestimates the U atomic charge by 0.50 electron. For this reason we recalculated the NPA charge assuming the 6d to be valence orbitals for all the oxy actinide cations.

For the ligands (alone) closed-shell ab initio calculations were performed at the MP2/6-311+g(2df,2p) level; open-shell calculations are not needed, as checked at the B3LYP/6-31+g(d,p) level. All the quantum calculations were done with the Gaussian98 and 03 suites of programs [23,24].

$\Delta_r E$, the ab initio energy, was calculated for the protonation reaction corresponding to the pK_a equilibrium (Fig. 3). pK_a represents $pH_{1/2}$; similarly, when adding
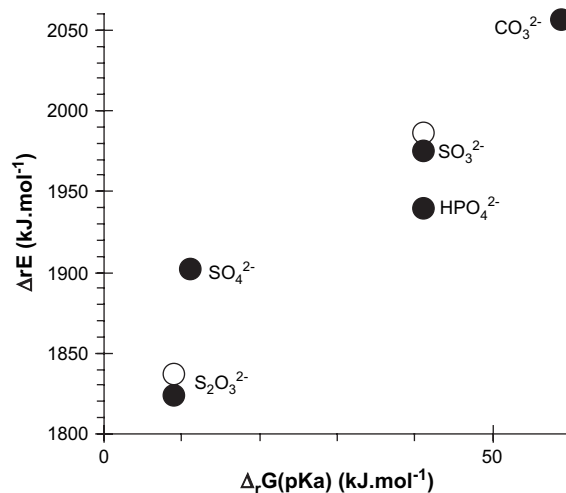
Fig. 3. Protonation reactions of RO_2^{2-} ligands in the gas phase and in aqueous solutions. The pK_a (in pure liquid water at 25 °C) are converted to kJ mol^{-1} ($\Delta_r G = -RTpK_a$) and compared to the energy of the corresponding reaction ab initio calculated (with neither matrix nor temperature correction), where the protonation is on an O (black points) or S (white points) atom.

AnO_2^{X-4} cations are not in the middle of the correlation cloud, indicating that the relevant phenomenological charge might be higher (than the formal one). Conversely, the corresponding points are moved to the other side of this correlation plot (not represented on the
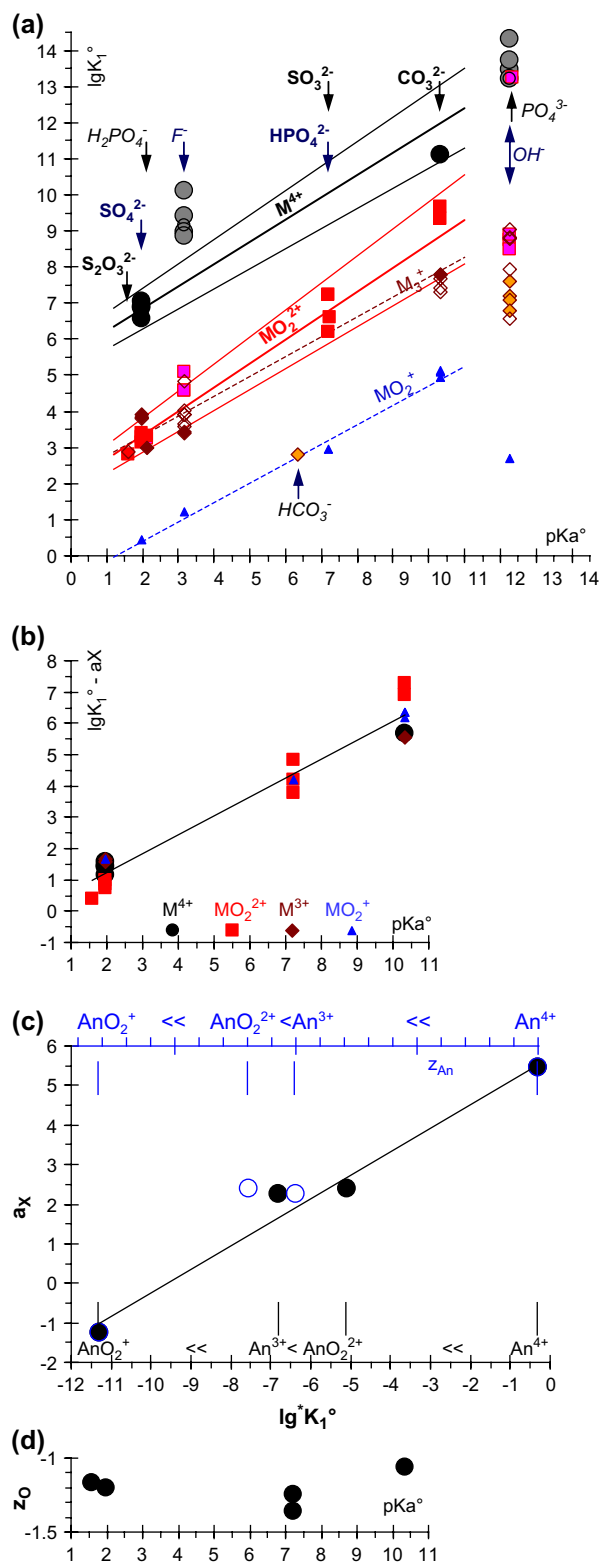
the entropic contribution to $\Delta_r E$, it represents $P_{H_{1/2}^+}$, the H^+ partial pressure: the hydration energy of H^+ is related to the slope in the $\Delta_r E$ plot as a function of pK_a (Fig. 3), while the intercept rather reflects the hydration energy change between the reactants and products. Since the slope is much greater than 1, the E scale had to be contracted, which means that the final correlation is quite poor. Slope $\neq 1$ also means it is not equivalent to use pK_a or $\Delta_r E$ for our estimates of complexing constants: pK_a appeared to be better correlated with measured complexing constants. Furthermore pK_a represents a marginal value of $\Delta_r E$, which already is a marginal part of the DFT calculated electronic energy: the experimental pK_a values are more reliable for our purpose and more accurate than the $\Delta_r E$ ones obtained from quantum calculations in the gas phase.

3. Results and discussions

3.1. Comparing the affinities of hard anions for H^+ and AnO_2^{2+}

We first examined U(VI) aqueous complexation and hydrolysis data, since a sufficiently large set of complexing constants is available. Positive $\log K_1^\circ$ vs pK_a° correlations are observed, and even linear correlations appear to fit the data reasonably well. The plot appeared to be less scattered when restricted to the consistent set of data selected by the NEA-TDB reviews (Fig. 4): we finally used these (NEA-TDB) consistent sets of data for the figures and numerical correlations given in the present paper with the following exceptions. For An(VI) we did not use the NEA-TDB PuO_2CO_3(aq) formation constant based on only ($\log K_1^\circ = 13.8_{-0.6}^{+0.8}$ [26] and 9.3 ± 0.5 [27]) two experimental determinations that are not consistent (within uncertainties). The latter

Fig. 4. Proton and other cation affinities for ligands. K_1° is the standard formation constant of the $ML^{z_M + z_L}$ complex, and K_a° is the protonation constant of the L^{z_L} ligand written on the figure (Table 1). Since all the ($\log K_{1,X}^\circ = a_X + b_X pK_a^\circ$) lines are virtually parallel for all the (X) oxidation states (a). We also used the same ($b_x = 0.62 \pm 0.16$) slope in $\log K_{1,X-a_X}^\circ = ((0.62 \pm 0.16)pK_a^\circ)$ regressions for the RO_2^{2-} ligands, and shifted the curves by a_x (b): $a_X - a_{VI} = (\log K_{1,X}^\circ - \log K_{1,VI}^\circ) = \log K_{X/VI}^\circ$ (Eq. (5)), where $K_{X/VI}^\circ$ is the constant for the $AnO_2RO_2/MRO_2^{z_M - 2}$ exchange equilibrium (Eq. (6a)) for $M^{z_M} = An^{3+}$, An^{4+} or AnO_2^+ For An at the oxidation state X, $a_X (= \log K_{1,X}^\circ - 0.62 pK_a^\circ)$ can be used as a definition of a quantitative scale for the (up to now qualitative) $An^{4+} > AnO_2^{2+} \approx An^{3+} > AnO_2^+$ series (y axis of (c)). It is compared (black filled symbols) with the hydrolysis constant ($^*K_1$) scale on the x axis (of (c)), and z_{An}, the An atomic charge (blue open symbols corresponding to the top scale). z_O, the atomic charge of O in RO_2^{2-} is not specially correlated with its pK_a (d).The x-axes are the same for (a), (b) and (d): the names of the ligands are only written on (a).

value (that we published ourselves) is closer to the U(VI) and Np(VI) ones (Table 1) [2,4], but it is rather a maximum possible value corresponding to the detection limit of our solubility measurements. For this reason, we also do not rely on the 9.5 ± 0.5 similar value more recently updated by the NEA-TDB review [16].

The PO_4^{3-} tri-anion is out of the correlation, while the F^- mono anion could probably be included into the correlation, but HO^- cannot (Fig. 4). When restricting the correlations to $L^{z_L} = RO_2^{2-}$ potentially bidentate oxygen-donor ligands, virtually the same $\log K_1^\circ$ value is observed for a given ligand with AnO_2^{2+} for $An = U$, Np, Pu or Am: the variations along this series are only slightly higher than experimental uncertainties. $\log K_{1,VI}^\circ = ((2.0 \pm 0.3) + (0.66_5 \pm 0.08_5) \ pK_a^\circ)$ is obtained for these (AnO_2^{2+}) cations. Adding not critically reviewed $(\log K_{1,VI}^\circ)$ values gives similar regression coefficients with increased uncertainties, namely (2.6 ± 0.8) instead of (2.0 ± 0.3), and (0.58 ± 0.08) instead of $(0.66_5 \pm 0.08_5)$.

3.2. $AnO_2RO_2/MRO_2^{z_M - 2}$ exchanges for $M^{z_M} = An^{3+}$, An^{4+} or AnO_2^+

Similar $\log K_1^\circ$ vs pK_a° correlations and observations (as for AnO_2^{2+}, Section 3.1) are made for the An^{3+} and AnO_2^+, cations, while there are too few data for M^{4+}.

For the M^{3+}/CO_3^{2-} systems, we used our own complexing constants (Table 1) [28], $AmHCO_3^+$ is an outlier, in part due to the stabilisation of H_2CO_3 as $CO_2(aq)$: the measured pK_a (of the $HCO_3^-/CO_2(aq)$ couple) is not the relevant parameter for our correlations. For $L^{z_L} = RO_2^{2-}$ we found K_1° values in the order $An^{4+} > AnO_2^{2+} \approx An^{3+} > AnO_2^+$, a classical order for the reactivity of actinide cations toward hard anions. However, $AnO_2^{2+} \geq An^{3+}$ is often written (instead of $AnO_2^{2+} \approx An^{3+}$). Here the available data for An^{3+} appear to be within the correlation lines of AnO_2^{2+}. The atomic charge of U in UO_2^{2+} is 2.8 electron, which compares with the charge of Am^{3+}. Nevertheless, using atomic charges in the correlations gave poorer results (see below and Fig. 4(c)). We obtained $\log K_{1,III}^\circ \approx 2.2 + 0.55 \ pK_a^\circ$ for An^{3+} and $\log K_{1,V}^\circ \approx -0.7 + 0.54 \ pK_a^\circ$ for AnO_2^{2+}.

There are too few data for a statistical evaluation of all the uncertainties. Nevertheless, it seems that b_x, the slopes (of every $\log K_1^\circ$ vs pK_a° correlations) are the same within uncertainties. Indeed a reasonable fit is obtained when fixing $b_x = b_{VI}$ $(= 0.66_5)$, namely $\log K_{1,X}^\circ = (a_X + 0.66_5 \ pK_a^\circ)$ for all the oxidation states. We finally fitted the slope (and a_x) on all the data, and obtained $\log K_{1,X}^\circ = (a_X + (0.61_6 \pm 0.05_5) \ pK_a^\circ)$ with $a_{III} = 2.25_3 \pm 0.07_5$, $a_{IV} = 5.44_4 \pm 0.24_9$, $a_V = -1.23_6 \pm 0.48_9$ and $a_{VI} = 2.40_8 \pm 0.45_3$ fitted

Table 1
Formation constants used to draw Fig. 4: pK_a° of RO_2^{2-} ligands and corresponding $K_{1,X}^\circ$ formation constants[c] with cations of f-block elements [2–4,16]

RO_2^{2-}	pK_a[b]	$\log K_{1,III}^\circ$ [c]	$\log K_{1,IV}^\circ$ [c]	$\log K_{1,V}^\circ$ [c]	$\log K_{1,VI}^\circ$ [c]
$S_2O_3^{2-}$	1.59		6.6 ± 0.8[a]		2.8(U)
			6.58(U)		3.15(U)
SO_4^{2-}	1.98	3.85(Am)	6.85(Np)	0.44(Np)	3.28(Np)
		3.91(Pu)	6.89(Pu)		3.38(Pu)
HPO_4^{2-}	7.21_2		$9._5 \pm 2._3$[a]	2.95(Np)	7.24(U)
					6.2(Np)
SO_3^{2-}	7.22		$9._5 \pm 2._3$[a]		6.6(U)
CO_3^{2-}	10.32_9	7.7 ± 0.3(Am)	$11._1 \pm 3._2$[a]	4.96_2(Np)	9.67(U)
		7.8 ± 0.2(Eu)		5.12(Pu)	9.32(Np)
				5.1(Am)	
a[d]		2.2	5.8 ± 0.4	−0.7	2.0 ± 0.3
b[d]		0.55	$0.5_1 \pm 0.2_7$	0.54	$0.66_5 \pm 0.08_5$
a_x[e]		$2.25_3 \pm 0.07_5$	$5.44_4 \pm 0.24_9$	$-1.23_6 \pm 0.48_9$	$2.40_8 \pm 0.45_3$
$\log K_{X/VI}^\circ$		$-0.1_6 \pm 0.5$	$3.0_4 \pm 0.5$	$-3.6_4 \pm 0.5$	0
$\log {}^* K_{X/VI}^\circ$		−1.7	4.81	−6.2	0

[a] Value estimated in the present work.

[b] pK_a of the RO_2^{2-} ligand.

[c] $K_{1,X}^\circ$ is the standard constant of equilibrium $M^{z+} + RO_2^{2-} \rightleftharpoons MRO_2^{(z-2)+}$ for $M^{z+} = An^{x+}$ ($X = 3$ or 4) or $AnO_2^{(X-4)+}$ ($X = 5$ or 6) from published data (see text) [2–4,7].

[d] a and b, the coefficients of the $\log K_{1,X}^\circ = (a + b \ pK_a^\circ)$ linear regression are fitted for a given oxidation state, X.

[e] while a_x is the (fitted) intercept of a similar regression, but with the same (0.62 ± 0.16) slope for all the oxidation states: $\log K_{1,X}^\circ - a_x = ((0.62 \pm 0.16) pK_a^\circ)$.

values, where uncertainties are 1.96σ (the maximum errors on $\log K^\circ_{1,X}$ was $+0.9$ for UO_2CO_3 and -0.8 for $AnCO_3^+$). Since there are not enough data for a meaningful statistical analysis, we finally increased the uncertainties: $\log K^\circ_{1,X} - a_X = (0.62 \pm 0.16)pK^\circ_a$ (Fig. 4(b)). The standard deviation of the fit is 0.5 (it represents less than 3 kJ mol^{-1}), a value only a little higher than that of many direct experimental determinations in aqueous solutions, and of the order of magnitude of the variations of the $\log K^\circ_1$ values among the series of the analogous cations considered here. However, when a slope is fitted for each oxidation state, a small systematic deviation can be inferred, namely the slopes seem slightly different for each type of central cation (AnO_2^{2+}, An^{3+} and AnO_2^+). On the other hand, this difference is small as compared to the scatter in the available data, and it is not specially correlated with the charge of the cation.

Since the (0.62 ± 0.16) slope does not depend on X, $(a_X - a_{VI}) = \log K^\circ_{X,VI}$ (Eq. (5)), the shift between the lines in Fig. 4(a) is related to the following equation:

$$AnO_2RO_2 + M^{z_M} \rightleftharpoons MRO_2^{z_M-2} + AnO_2^{2+} \qquad (6a)$$
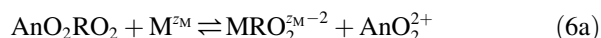
$AnO_2RO_2/MRO_2^{z_M-2}$ exchange equilibrium (Eq. (5)) whose equilibrium constant is $K^\circ_{X/VI}$. For such anions the order of their reactivity toward H^+ and actinide ions is found to be

$$CO_3^{2-} > HPO_4^{2-} \approx SO_3^{2-} > SO_4^{2-} \geq S_2O_3^{2-}$$

also corresponding to their pK°_a values, but not specially to z_O, the atomic charge of O (Fig. 4(d)).

We also attempted to force $b = 1$ in the fits, but without success: the correlations cannot simply be interpreted with Eq. (4).

Similarly, hydrolysis equilibria were compared using $^*K^\circ_{X/VI}$ (Eq. (8)), the constant of a hydrolysis competition equilibrium (Eq. (7)) between actinide ions at oxidation states X and $+6$: $\log {}^*K^\circ_{III/VI} = -1.7$, $\log {}^*K^\circ_{IV/VI} = 4.81$ and $\log {}^*K^\circ_{V/VI} = -6.2$ for Np [4]. These results give nearly the same $An^{4+} >> AnO_2^{2+} > An^{3+} >> AnO_2^+$ qualitative scale (Fig. 4(c)), and the $\log {}^*K^\circ_{X/VI} = (0.36 + 0.60)\log {}^*K_{X/VI}$ linear correlation.

3.3. Estimating the stabilities of $An^{(IV)}RO_2^{2+}$ complexes

We now want to estimate missing complexing constants for U(IV), namely with the SO_3^{2-} and $S_2O_3^{2-}$ anions. For this we could not use the same type of correlations as those observed for UO_2^{2+} and the other cations (Section 3.2), because reliable formation

constant has been published for only one type of 1:1 An(IV) complexes, namely for the MSO_4^{2+} complexes: $\log K^\circ_{1,IV} = 6.58$ (USO_4^{2+}) [2], 6.85 ($NpSO_4^{2+}$) [4], 6.89 ($PuSO_4^{2+}$) [4] and 7.04 ($ZrSO_4^{2+}$) [15]. When using this single datum and the (0.62 ± 0.16) slope value estimated above, the $(\log K^\circ_{1,IV} = ((5.6 \pm 0.2) + (0.62 \pm 0.16) pK^\circ_a)$ line is drawn, from which $\log K^\circ_{1,IV} = (12.0 \pm 1.9)$, (10.1 ± 1.4), (6.8 ± 0.5) and (6.6 ± 0.5) are calculated for the An(IV) complexes of CO_3^{2-}, SO_3^{2-}, SO_4^{2-} and $S_2O_3^{2-}$, respectively. The value of $a_{IV} = 5.6 \pm 0.2$ was chosen to fit the 6.58 (USO_4^{2+}), 6.85 ($NpSO_4^{2+}$) and 6.89 ($PuSO_4^{2+}$) data by giving less weight to USO_4^{2+}, because the $+4$ oxidation state is more difficult to stabilise for uranium, even if more experimental studies of U(IV) are available. However, the $\log K^\circ_{1,IV}$ ($=6.6 \pm 0.5$) $MS_2O_3^{2+}$ value is close to the MSO_4^{2+} fixed point (of the correlation). Therefore it does not depend sensitively on the value estimated for the slope (of the $\log K^\circ_{1,IV}$ vs pK°_a linear correlation). Consequently the uncertainties are relatively small for (the $\log K^\circ_{1,IV}$ estimate of) $MS_2O_3^{2+}$. Conversely the biggest uncertainty is for MCO_3^{2+} the most stable complex, since CO_3^{2-} appeared to be the most reactive RO_2^{2-} ligand we studied: it is one of the endpoints of the correlation lines. For this reason, we estimated an upper bound for the value of $\log K^\circ_{1,IV}$ from experimental data: we re-interpreted available published experimental solubilities of actinides(IV) by using the same methodology as in Refs. [4,5,29]. We obtained formation constants consistent with the original interpretation (by the authors of Ref. [9]). However, for consistency we added the known stabilities of $An(CO_3)_i^{4-2i}$ ($i = 4$ and 5), and we tested many possible complexes for which we also estimated maximum possible stabilities (Table 2) for sensibility analysis; our purpose was essentially to estimate a value for $AnCO_3^{2+}$. As expected from pH vs $\log [CO_3^{2-}]$ predominance diagrams [7,26,28], the most restrictive conditions were found for published solubilities of An(IV) measured at low pH and high CO_2 partial pressure, namely in Refs. [9,30]. In both cases we obtained virtually the same values: $\log K^\circ_{1,IV} \leq 11.1$ or 11.5 for the $ThCO_3^{2+}$ complex. Using this value (and the sulfate data), $\log K^\circ_{1,IV} = (5.8 + 0.51 pK^\circ_a)$ is calculated, from which $\log K^\circ_{1,IV} = 11.1$, 9.5, 6.8 and 6.6 are calculated for the An(IV) complexes CO_3^{2-}, SO_3^{2-}, SO_4^{2-} and $S_2O_3^{2-}$, respectively. These values are within the uncertainties of the previous estimates above. The $AnCO_3^{2+}$ value of 11.1 is identical as, or slightly smaller (by 0.9 ± 1.9) than the central value (12.0 ± 1.9) of the above estimate, and the same trend was observed for $AmCO_3^+$: it was overestimated by $0.8 \log_{10}$ unit when using the

Table 2
Stabilities of An(IV) carbonato complexes

An(CO$_3$)$_i$(OH)$_j^{4-2i-j}$	log $K_{i,j}^{\circ}$(Pu)[a] [5]	log $K_{i,j}^{\circ}$(Th)[a] [9]	log $K_{i,j}^{\circ}$(Th)[a,b]
AnOH^{3+}	13.2		
AnCO$_3^{2+}$			≤11.1
AnCO$_3$OH$^+$			<21.1
An(CO$_3$)$_2$			<20.8
AnCO$_3$(OH)$_2$	<<42	27.0	<30.1
An(OH)$_4$	<<47.$_9$		38.5
An(CO$_3$)$_2$OH$^-$	<<40.$_5$		<29.4
AnCO$_3$(OH)$_3^-$	<<47.$_7$	34.8	≤38.5
An(CO$_3$)$_3^{2-}$	<<37.$_6$		<27.5
An(CO$_3$)$_2$(OH)$_2^{2-}$	<<46.$_2$	33.3	≤36.8
AnCO$_3$(OH)$_4^{2-}$	<<51.$_8$	37.4	≤39.9
An(CO$_3$)$_3$OH^{3-}	<<42		≤34
An(CO$_3$)$_2$(OH)$_3^{3-}$	<<50.$_5$		<39.2
An(CO$_3$)$_4^{4-}$	37		29.9
An(CO$_3$)$_3$(OH)$_2^{4-}$	<41		<37.6
An(CO$_3$)$_3$(OH)$_3^{5-}$	<40.$_5$		<37.9
An(CO$_3$)$_4$OH^{5-}	<39	34.4	35.4
An(CO$_3$)$_5^{6-}$	35.$_6$		28.4
An(CO$_3$)$_4$(OH)$_2^{6-}$	<37		<36.4
An(CO$_3$)$_3$(OH)$_4^{6-}$	<38.$_5$		<39.3
An(CO$_3$)$_6^{8-}$			<36

[a] $K_{i,j}$ is the standard constant of equilibrium An^{4+} + iCO$_3^{2-}$ + jHO$^- \rightleftharpoons$ An(CO$_3$)$_i$(OH)$_j^{4-2i-j}$.

[b] Maximum possible values from the experimental data of Ref. [9]; these estimations are consistent with the original interpretation (by the authors of Ref. [9]), but the known stabilities of An(CO$_3$)$_i^{4-2i}$ are here added in the fits for $i = 4$ and 5; our purpose was essentially to estimate a value for AnCO$_3^{2+}$ (see text) and to outline sensitivity analysis.

same slope (0.62) for all oxidation states. This correlation predicts under-stabilisation of the AnCO$_3^{X-2}$ complexes ($X = 3$ or 4) as compared to the AnO$_2$CO$_3^{X-6}$ systems ($X = 5$ or 6): it might be attributed to the planar structure of CO$_3^{2-}$, which offers a better fit to the geometry of the coordinating equatorial plane of the AnO$_2^{X-4}$ actinyl cations. Unfortunately, such an explanation would also hold
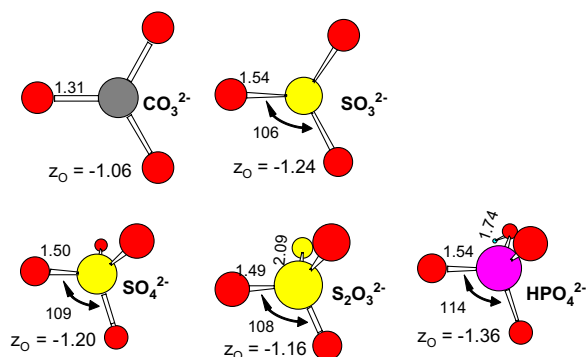
Fig. 5. Geometry of RO$_2^{2-}$ ligands optimized in the gas phase. R–O bond distances (Å), angles (°) and z_O, the atomic charge of O are written on the figure.

for the SO$_3^{2-}$ (quasi-) planar ligand (Fig. 5), which is not specially confirmed (Fig. 4). For consistency with our estimate, log $K_{1,\text{IV}}^{\circ} \leq 11.1$, we prefer the last correlation log $K_{1,\text{IV}}^{\circ} = (5.8 + 0.51 \ \text{p}K_a^{\circ})$, where we increased the uncertainties to encompass the previous log $K_{1,\text{IV}}^{\circ} = ((5.6 \pm 0.2) + (0.62 \pm 0.16)\text{p}K_a^{\circ})$ correlation: log $K_{1,\text{IV}}^{\circ} = ((5.8 \pm 0.4) + (0.5_1 \pm 0.2_7) \ \text{p}K_a^{\circ})$ from which we obtain log $K_{1,\text{IV}}^{\circ} \leq 11._1 \pm 3._2$ for AnCO$_3^{2+}$, $= 9._5 \pm 2._3$ for AnSO$_3^{2+}$, $9._5 \pm 2._3$ for AnHPO$_4^{2+}$ and 6.6 ± 0.8 for AnS$_2$O$_3^{2+}$, where uncertainties are increased take into account the lack of experimental data.

log $K_{1,\text{IV}}^{\circ} = 6.6 \pm 0.8$, the value estimated for AnS$_2$O$_3^{2+}$ is quite similar to those for the AnSO$_4^{2+}$ complexes: 6.58 (USO$_4^{2+}$), 6.85 (NpSO$_4^{2+}$) and 6.89 (PuSO$_4^{2+}$). This is consistent with the molecular structures of these ligands: SO$_4^{2-}$ and S$_2$O$_3^{2-}$ both have a tetrahedral structure (Fig. 5) – an O atom (of SO$_4^{2-}$) being replaced by an S atom (in S$_2$O$_3^{2-}$) and similar pK_a values. SO$_3^{2-}$ has a different structure, a higher pK_a, and a higher estimated value of the complexation constant. Unfortunately, it does not seem easy to draw any simple explanation just from z_O, the atomic charge of the free ligand in vacuum (Fig. 4(d)).

3.4. Uranium geochemistry

In non-complexing aqueous solutions, the solubility of uranium is controlled by uraninite (UO$_2$(s)) in reducing conditions, and by schoepite (UO$_3$(s)) in oxidizing and neutral conditions, as illustrated in Fig. 6(a) for 1 μM [U]$_t$. Besides those minerals, aqueous U(VI) species are predominant in a large E–pH domain, while aqueous U(IV) is stable only in reducing conditions, and is mostly hydrolysed.

On adding carbonate ions at a typical concentration of underground waters, aqueous U(VI) carbonate complexes prevail between pH 4 and 12 (Fig. 6(b)), UO$_3$(s) is totally dissolved, and the UO$_2$(s) stability domain is reduced. We have ignored the reduction of the carbonate ions, since this reaction is usually very slow. Nevertheless, no carbonate complex of U(IV) appears on the Pourbaix diagrams. These complexes would predominate only at higher carbonate concentrations than those studied here. Rai and Ryan have already proposed that carbonate complexation of actinide(IV) ions in environmental conditions can be neglected [8].

Among the main sulfur species, SO$_4^{2-}$ prevails over a large (E–pH) domain in oxidizing to slightly reducing equilibrium conditions. For high pH values, this domain even extends to reducing conditions (Fig. 1). H$_2$S, HS$^-$ and S^{2-} prevail in reducing conditions, but their
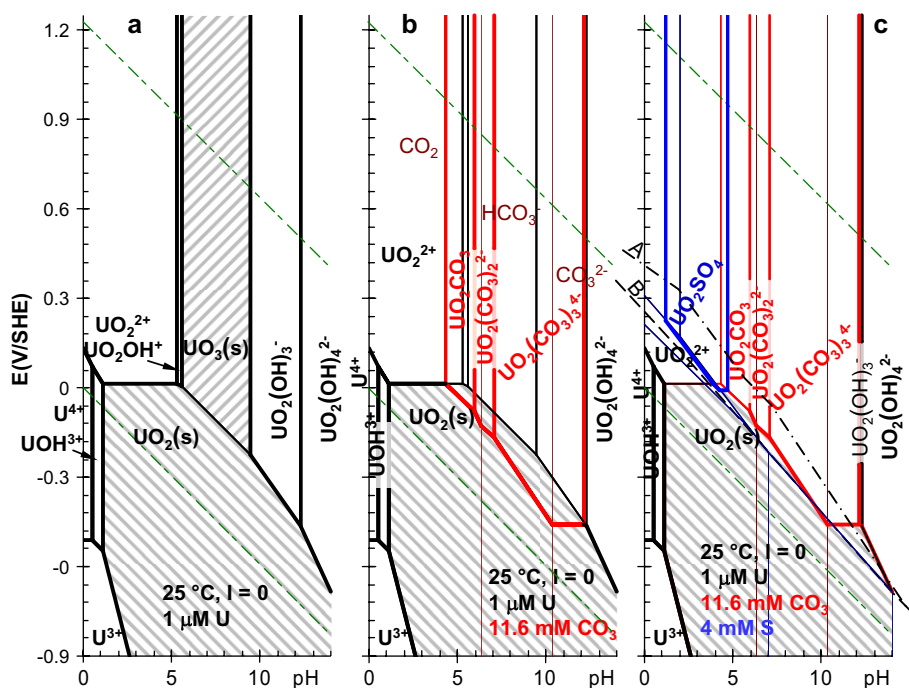
Fig. 6. Pourbaix' diagrams of uranium. The predominance domains of the major soluble species are shown as a function of pH and E, the redox potential of the solution in (a) non-complexing media, (b) adding the influences of carbonate ions and (c) sulfur species for a typical ($[CO_3]_t = 11.6$ mM and $[S]_t = 4$ mM) composition of underground waters [11]. pH is taken into account for carbonate speciation ($CO_3^{2-}/HCO_3^-/CO_2(aq)$), but its reduction -typically into $CH_4(g)$- is not. The mixed dashed line (A) represents redox conditions in Fig. 7. The long dashed line (B) represents redox conditions for Fig. 1(c).

complexing properties are not significant for the (hard) cations of the f-block elements. $UO_2SO_4(aq)$ is the only predominating sulfur species in our typical underground water conditions (Fig. 6(c)), even when introducing the 1:1 complexing constants estimated above (Section 3.3, Table 1) for $US_2O_3^{2+}$ and USO_3^{2+}. The RO_2^{2-} ligands are protonated in acidic conditions, which decreases their concentrations: the corresponding 1:1 complexing equilibria are actually the

$$M^{z_M} + HRO_2^- \rightleftharpoons MRO_2^{z_M-2} + H^+ \qquad (4a)$$
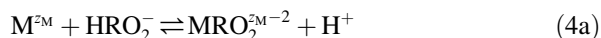
exchange equilibria. Despite this concurrency between protonation and complexation, several complexes with the 1:1 stoichiometry are stable. Conversely, the existence of $AnCO_3^{2+}$ complexes has never been demonstrated, since the competition (between carbonate complexation and hydrolysis) is less favourable for An(IV) as compared to the actinides in the other oxidation states (Fig. 4(a)). The RO_2^{2-} concentration can also dramatically decrease as a result of redox reactions: CO_3^{2-} and $SO_4^{2-}(= RO_2^{2-})$ are reduced in equilibrium chemical conditions, where U(IV) is stable. However, these reduction reactions are very slow: we have

neglected them for the carbonate ions (Fig. 6). Similarly, the coexistence of S(VI) and S(−II) species is often observed, indicating that equilibrium conditions are not always achieved for S natural aqueous systems. The achievement of the U(IV)/U(VI) equilibrium can also last for a few weeks. Note that all these slow reduction reactions can be explained by the need to break strong (covalent) bonds of O(−II) with C, S(VI) or U(VI). Such kinetics is often handled by assuming that slow reactions are blocked, while equilibrium conditions are achieved for other equilibria. Therefore U(IV) might be complexed by sulfate and by reduced intermediary S species as well: we plotted two simulation diagrams corresponding to different kinetic assumptions that would stabilise sulfoxy-anion complexes (Fig. 7). In both cases, E, the redox potential, is at the limit of the $H_iS_2O_3^{i-2}$ and $H_iSO_3^{i-2}$ domains as plotted in Fig. 1(a) and line A in Fig. 6(c). In such redox conditions uranium aqueous species are stable at the +6 oxidation state. For this reason, the sulfate complexes of U(IV) are not seen on the Pourbaix' diagram (Fig. 6(c)): the sulfate ions are reduced in equilibrium conditions, where U(IV) aqueous species are dominating − i.e. the S(VI)/S(−II) frontier (line B in Fig. 6(c)) is at higher
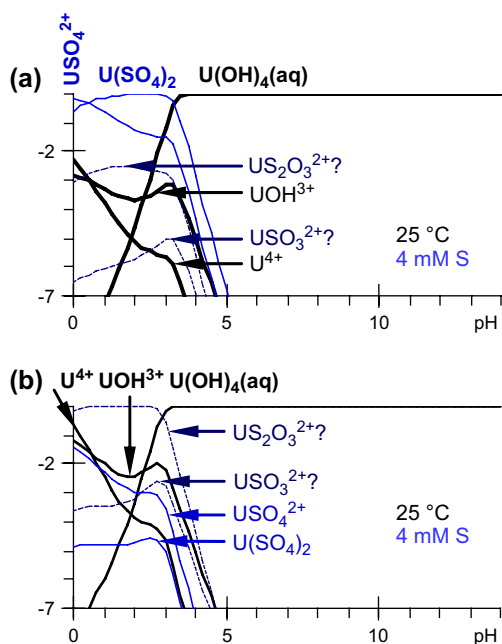
Fig. 7. Distribution of aqueous U(IV) species. $\lg(|A|/|U(IV)|)$ is plotted as a function of pH, where $|A|$ is the activity of an aqueous U(IV) species. The conditions are the same as in Fig. 6(c) except for E, the redox potential of the solution: $H_iSO_4^{i-2}$ (a) or $H_iS_2O_3^{i-2}$ (b) are assumed to be the major S species. $[H_iS_2O_3^{i-2}]/[H_iSO_3^{i-2}] \approx 10$ (mixed dashed line A in Fig. 6(c)). $[H_iSO_4^{i-2}]/[H_iS_2O_3^{i-2}] \approx 20$ (a) or ≈ 1 (b) corresponding to different kinetic assumptions.

potentials than the U(VI)/U(IV) frontier in most pH conditions. Nevertheless we only focus on U(IV) aqueous species; therefore they would be minor uranium species, when the U(VI)/U(IV) equilibria are achieved.

In a first simulation we assumed that the major S species are in the +6 oxidation state (namely $H_iSO_4^{i-2}$), and that $[H_iSO_4^{i-2}]/[H_iS_2O_3^{i-2}] \approx 20$, which corresponds to much higher $H_iS_2O_3^{i-2}$ concentrations than in equilibrium conditions (for kinetic reasons). The USO_4^{2+} and $U(SO_4)_2$ sulfate complexes still appear to be U(IV) major species in acidic conditions (pH < 3.2), while nearly 1% of $US_2O_3^{2+}$ can be formed (Fig. 7(a)). Yet $US_2O_3^{2+}$ might be a kinetic intermediate, since uraninite is often associated with pyrite (FeS$_2$); indeed $S_2O_3^{2-}$ is an intermediary product of its oxidative dissolution [14]. $S_2O_3^{2-}$ and SO_4^{2-} have similar reactivities (Fig. 4), but (in our hypothesis) the SO_4^{2-} concentration is higher (than the $S_2O_3^{2-}$ one), which explains why the sulfate complexes dominate. Although the SO_3^{2-} ions are more reactive, the USO_3^{2-} complex is negligible in that simulation, since the reduction of SO_3^{2-} (Fig. 1) decreases its concentration and consequently its complexing ability.

In a second simulation we assumed that SO_4^{2-} is not formed at all (still for kinetic reasons). Therefore $S_2O_3^{2-}$

is now the dominating S aqueous species (Fig. 1). $US_2O_3^{2+}$ is the major U(IV) species, and up to a few percent of USO_3^{2+} is formed at pH less than 3.0 (Fig. 7(b)).

Even if sulfoxy-anions complexes of U(IV) are certainly not stable in equilibrium conditions, these simulations indicate that they might be formed as kinetic intermediates typically in the course of uraninite and pyrite oxidative dissolutions, or the interaction of aqueous uranium (including U(VI)) with pyrite surfaces [31,32]. Of course, this statement needs experimental confirmation, specially in less acidic to basic conditions, where higher and mixed $An(RO_2)_i(OH)_j^{4-2i-j}$ complexes may form. Furthermore, at pH > 3, $U(OH)_4$(aq) is the dominant species in equilibrium reducing conditions, and the formation of S-containing complexes is less favourable, specially in the usual pH conditions of equilibrated natural under-ground-waters.

3.5. Hydrolysis of actinide ions

We now consider where protactinium should be placed in the above correlations. There is little experimental published information on Pa aqueous chemistry. We first used the available information on its aqueous species in non-complexing (acidic) solutions and its hydrolysis. Although Pa is known to be an f-block element [17], Pa(V) aqueous chemistry is closer to that of d elements (in the same — the 5th- column of the periodic table) than to the chemistry of AnO_2^+ trans-protactinian actinide cations. Here is a strong indication that PaO_2^+ is not the dominating aqueous Pa species.

Jaussaud et al. recently reviewed previous measurements of the Pa(V) hydrolysis constants [33–35]. They are essentially based on liquid–liquid extraction measurements, for which they pointed out many experimental difficulties: side reactions of the organic chemicals, sorption of Pa(V) on vessels and unwanted side reactions. Surprisingly most of the published studies are only based on measurements at trace concentrations of Pa(V), while sorption reactions are classically made negligible by using (non-radioactive) chemical analogues at macro-concentrations. The hydrolysis behaviour of Nb(V) seems similar to that proposed for Pa(V): we calculated the hydrolysis constants of Nb(V) by interpreting the aqueous solubility of Nb$_2$O$_5$ (Table 3) [25]. We re-interpreted the (Pa) experimental measurements at 25 °C by giving more weight to the data for which systematic errors seemed the lowest according to Jaussaud's observations and comments: the measurements at high ionic strength and low (TTA = thenoyltrifluoroacetone) extractant concentrations. This essentially confirmed the original interpretation

Table 3
Pa(V) hydrolysis constants

I (M)	$\log {}^*K_{1,m}{}^e$	$\log {}^*K_{2,m}{}^e$	$\log {}^*K_{3,m}{}^e$	
3		-2.0 ± 0.15	-5.8 ± 0.3^b	[33−35]
3	-0.35 ± 0.29	-1.75 ± 0.91	< -3.5	[33][a]
1		-1.7 ± 0.2	-6.9 ± 0.6^b	[33−35]
1	$\geq -0.38^c$	-1.50 ± 0.56	$< -0.98^b$	[33][a]
0.5		-1.6 ± 0.2	-6.9 ± 0.6^b	[33,35]
0.5		-1.49^c		[33][a]
0.1		-1.5 ± 0.2	-7.0 ± 0.6^b	[33−35]
0.1		-1.80 ± 0.34		[33][a]
0.1	$\geq -0.75^c$	-1.65 ± 0.2	-4.95 ± 0.2	Nb(V)[d] [36][a]
0		-1.24 ± 0.02	-7.03 ± 0.15^b	[33,35]
0		-1.26 ± 0.15	-7.15 ± 0.4^b	[34]
0	-0.04 ± 0.36^c	-1.44 ± 0.71	$< -3.6^c$	[33][a]

One value is also tabulated for Nb(V).

[a] Graphically interpreted in the present work, and (last line) extrapolated to $I = 0$. See Fig. 8.

[b] Inconsistent value: since the measurements were performed at pH < 4, it is not possible to fit (from them) a $\log K_i$ value less than about −4.

[c] There is no clear experimental evidence of the corresponding reaction.

[d] Nb(V) value fitted from solubility data [36], and here tabulated for comparison.

[e] $K_{i,m}$ is the constant of equilibrium PaO.

Fig. 8. Predominance diagram of Pa(V) hydrolysis species. The hydrolysis constants ($-\log {}^*K_1^\circ = \mathrm{pH}_{1/2,i}$ correspond to the pH value at the half-point reaction) have been re-interpreted (Table 3) from the experimental data (and extrapolated to $I = 0$ with the SIT formula) of Ref. [30] in 0.1 (open symbols) to 3 (filled symbols of the same colour) mol L^{-1} NaClO$_4$ aqueous solutions for the successive formations of species of charges 2 (dark blue diamonds), 1 (brown circles) and 0 (green squares). The intermediate colours are for 1 and 0.5 mol L^{-1}. For higher [TTA] values (not represented), a systematic deviation is observed. (For interpretation of the references to colour in this figure legend, the reader is referred to the web version of this article.)

given by the authors, but increased uncertainties and suppressed an inconsistency (Table 3). Namely, classical slope analyses of the raw experimental data imply a Pa species of charge +1 in 0.1 M NaClO$_4$ aqueous solutions, and +2 at higher I (3 M), consistent with the PaOOH(OH)$^+$ and PaOOH^{2+} stoichiometries [17] in nearly the whole pH range studied (0 < pH < 4). Indeed, high I usually stabilizes the species of higher charges. There is no clear evidence for neutral and tricationic species, due to the scattering of the data (Fig. 8). A neutral Pa species is certainly formed, but it is clearly stabilized by increasing [TTA]$_t$, the total TTA concentration (results not reproduced in Fig. 8 for clarity), which suggests the corresponding aqueous Pa(V) species might include ionised deprotonated TTA ligands, which would hide the formation of PaOOH(OH)$_2$ (equivalently written PaO(OH)$_3$ or Pa(OH)$_5$). The formation of PaO^{3+} is not proposed in the original interpretation of the authors, and indeed needs confirmation. Finally, the most reliable published Pa(V) standard hydrolysis constant is certainly $\log {}^*K_2^\circ = -(1.26 \pm 0.15)$ [34], a value consistent with our re-interpretation (-1.44 ± 0.71) (Fig. 8 and Table 3), and with the Nb(V) value of $-(1.65 \pm 0.2)$. We also propose $\log {}^*K_1^\circ = -(0.04 \pm 0.36)$ and $\log {}^*K_3^\circ \ll -3.6$, giving no credit to the $(-(7.15 \pm 0.4)$ [34] and $-(7.03 \pm 0.15)$ [33,35]) published interpretations from

the same experimental data, because the corresponding hydrolysis species could not be detected in the experimental conditions used in this work (pH ≤ 4 corresponding to a maximum value of about $10^{-7+4} = 0.1\%$ for the concentration of the hydrolysis species to be compared with the $10^{0.71}$ uncertainty in the measurements of $\log {}^*K_2^\circ$), even though they might provide a reasonable value: the Nb(V) value of -4.95 ± 0.2 might also be used as a rough estimate. These ${}^*K_i^\circ$ constants are actually the hydrolysis constant of PaO^{3+}, but the existence of this species has not clearly been demonstrated, and for this reason only the second stepwise experimental determination $({}^*K_2^\circ)$ seems reliable, while the first one $({}^*K_1^\circ)$ needs confirmation. The $-\log {}^*K_2^\circ$ value is only a little larger than that of $-\log {}^*K_1^\circ$: the two first hydrolyses of Pa(V) would be nearly simultaneous. This is also observed for the other actinide aqueous species.

A linear regression correlates reasonably well $\log {}^*K_1^\circ$, the logarithm of the hydrolysis constant and z, the charge of the M^{z+} cation for M^{z+} = Ra^{2+}, Am^{3+}, Pu^{4+} (brown dotted line in Fig. 9(a)): $-\log {}^*K_i^\circ \approx (25.2_4 - 6.1_6 z)$. Adding other An^{3+} and An^{4+} cations gives virtually the same correlation (brown dotted line in Fig. 9(b)): $-\log {}^*K_i^\circ \approx (25.6_7 - 6.2_8 z)$. The actinyl ions such as UO$_2^{2+}$, and NpO$_2^+$ are below this correlation line. This stabilisation of their hydrolysed species might be originated in an An−O$_{yl}$ (intramolecular) charge transfer induced on approaching equatorial water
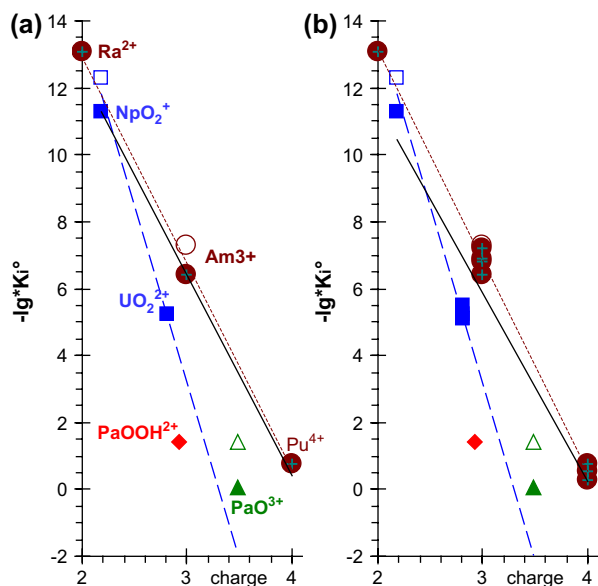
Fig. 9. Hydrolysis constants of actinide aqueous ions: $-\log {}^*K_1^{\circ}$ (filled symbols) and $-\log {}^*K_2^{\circ}$ (open symbols). The lines represent the linear regressions for (black line) all the points plotted on the figures excepted Pa(V) ones, only for the (Ra^{2+}, Am^{3+}, Pu^{4+}) set (brown dotted line), or only for the (NpO_2^+ and UO_2^{2+}) set (blue dashed line). The (atomic NPA) charges of the bare An cations (written in Fig. 9(a)) were obtained from DFT quantum calculations in gas phase. Data and corresponding lines are plotted by adding similar cations in Fig. 9(b). Two possible stoichiometries of "the" Pa(V) aqueous species are represented. (For interpretation of the references to colour in this figure legend, the reader is referred to the web version of this article.)

molecules to UO_2^{2+} [21], an inductive effects of O_{water}, which is expected to be more important for HO^- equatorial ligands (where O_{yl} is an O atom of an $AnO_2^{(X-4)+}$ actinyl cation, while O_{water} is an O atom of a water equatorial ligand of the actinyl). Nevertheless, the actinyl cations are not far from the correlation lines: including UO_2^{2+} and NpO_2^+ but excluding Ra^{2+} (black lines in Fig. 9); $-\log {}^*K_i^{\circ} \approx (24.4_3 - 6.0_1 z)$, and adding other AnO_2^{2+} and AnO_2^+: $-\log {}^*K_i^{\circ} \approx (22.7_3 - 5.6_2 z)$, while extrapolating (blue dashed lines in Fig. 9) the AnO_2^{2+} and AnO_2^+ data give (blue dashed) lines (in Fig. 9) that are between the PaO^{3+} and $PaOOH^{2+}$ data. Namely, PaO^{3+}(aq) would be intermediate between the bare actinide hard cations (An^{x+}, $X = 3$ or 4), and the usual actinyl cations ($AnO_2^{(x-4)+}$, $X = 5$ or 6, An = U, Np, Pu or Am), whose polarization by equatorial ligands essentially results in the intramolecular charge transfer between An and O_{yl}. Note that despite this polarization $AnO_2^{(X-4)+}$ is still a hard cation for the equatorial ligands — i.e. negligible charge transfer from the equatorial ligands — we may wonder whether assuming this concept of

(equatorial) hardness/(intra-actinyl) softness is still relevant for such a behaviour. However, the $AnO_2^+/AnO_2^{2+}/ PaO^{3+}$ set can as well be considered as a series of actinide oxo-cations on their own line (approximately the blue dashed one in Fig. 9). As a result of their polarizability, these oxo-cations are below the (brown dotted) line of the bare M^{z+} cations. This polarizibility probably decreases z_{An}, the An atomic charge (in the oxo-cation) by inductive effect. This inductive effect would increase with z_{An}: this can explain the quite surprisingly low calculated atomic charges of U (in UO_2^+) and Pa (in PaO^{3+}), which would therefore be at the origin of the more negative slope for the actinide oxo-cation line (as compared to that of the bare cations). However, this proposition needs confirmation, since the Pa(V) experimental results are neither very accurate, nor validated, and since physical explanations cannot be proven by only such empirical correlations: it is a limit of such correlations, rather than problems in the (very few) experimental data. According to this interpretation, two correlation lines are expected, one for the bare An^{x+} cations, and the other one for the $AnO_2^{(X-4)+}$ di-oxo-cations, while the PaO^{3+} mono-oxo-cation would fall between these lines, as we actually observed.

The experimental hydrolysis data already indicated that $PaOOH^{2+}$ should be only a little less reactive than Pu^{4+}. Finally, it can still be under debate whether it is better to consider PaO^{3+} or $PaOOH^{2+}$, or both, as the Pa(V) aqueous species. Using atomic charges here gave unexpected correlations, as compared to the other chemical studies reviewed in the present paper. Nevertheless, it is not a convincing proof that PaO^{3+} can be an important aqueous species (i.e. it is not a confirmation of the above estimate of its $-\log {}^*K_1^{\circ}$ value).

Our DFT calculations give pictures confirming that $PaOOH^{2+}$(aq) is a logical species, similar to UO_2^{2+}(aq), while PaO_2^+(aq) is easily protonated. $PaOOH^{2+}$ is merely protonated PaO_2^+ [17]. However, our continuing DFT calculations for interpreting published EXAFS measurements clearly indicate that the PaO^{3+} geometry exists in the Pa(V) species formed in concentrated H_2SO_4 aqueous solutions, since none of the other tested model geometries reproduced the shortest experimental distance, including $PaOOH^{2+}$: it thus dissociates in complexing media, to give aqueous sulfate complexes of PaO^{3+}.

4. Concluding remarks on analogies

($\log K_1^{\circ}$ vs pK_a°) correlations fit experimental data surprisingly well (Fig. 4(a)) for An(III to VI) complexes, with the exception of Pa(V), with 5 anionic

potentially bidentate and oxygen-donor RO_2^{2-} ligands: $CO_3^{2-} > HPO_4^{2-} \approx SO_3^{2-} > SO_4^{2-} \geq S_2O_3^{2-}$ in the order of their reactivities for the actinide cations. Furthermore, the correlations were found to be linear for each oxidation state, and the (0.62) slope of these H^+/An(X) correlations are approximately the same for all the oxidation states (X). This, of course, means that the An(X)/An(VI) correlations deduced are linear with slope 1: a_x, the intercept, is interpreted in terms of the half-reaction point, namely $10^{a_X - a_{VI}} = K_{1,X}^\circ / K_{1,VI}^\circ = K_{X/VI}^\circ$ (Eq. (5)) is the constant of the exchange equilibrium (Eq. (6a)), which takes (approximately) the same value (Table 1) for all the RO_2^{2-} ligands and for a given oxidation state. This provides a_x-based numerical values for the (up to now qualitative) scale $An^{4+} > AnO_2^{2+} \approx An^{3+} > AnO_2^+$ (Fig. 4(c)). The a_x values are also qualitatively correlated with z, the atomic charges of the An cations; but using z instead of a_x gives a poorer correlation (Fig. 4(c)). Note that measured energies of reactions, namely the hydrolysis constants of Pa(V), show clearly that it is not an analogue of the other An(V); quantum calculations give a chemical explanation of the destabilization of PaO_2^+ by hydration, typically resulting in clear apical H-bonded water molecules [17]. The two approaches are complementary: the experimental energies of reactions are more accurate, while quantum calculations provide geometries and other physical data that can be interpreted in terms of usual chemical concepts (atomic charges, bounds and their covalency…) for explaining the observed chemical reactivity.

All the correlations we used are totally empirical. They are probably the result of various effects, some of them more or less cancel out in the correlations, and they are probably all linked to z, the atomic charge of the cation. However, using z gave poorer linear correlations than comparing only experimental equilibrium constants. For this reason it is certainly better to interpret the correlations with chemical concepts than with any unproven physical explanation. Nevertheless, intramolecular charge transfers are deduced from quantum calculations for (possibly protonated) actinyl cations. These charge transfers can be related to the slightly different trends observed between the hydrolysis behaviours for these three types of cations (An^{z+}, PaO^{3+} and AnO_2^{X-4}). This effect would be a little less important for PaO^{3+} than for the AnO_2^{X-4} cations where there are more covalent bounds (which promote intramolecular charge transfer). Charge transfers might as well be at the origin of the over-stabilisation of the aqueous An(IV) hydroxides as compared to complexation. These predictions are restricted to similar complexes: the linear

regression numbers cannot be extended to all types of complexes without validations. Indeed such approaches exist in literature, overestimating the stabilities of several hypothetical chemical species, whose existences have never been confirmed; such numbers are not considered in the NEA-TDB reviews [2–4].

We have in fact used several levels of analogy giving different rules of thumb (although some have similar mathematical equations), which might indicate that it is hopeless to develop more general empirical formulae. The strongest analogy is typically for M(X), the series of An and other cations with the same charge, geometry and oxidation state, X: they form soluble complexes and hydroxides with the same stoichiometries, and with stability constant values that hardly differ by more than the experimental uncertainties. For different (X) oxidation states, linear correlations were found with slope 1, which defines a second type of analogy: considering the AnO_2^{2+}/M^{z_M} exchange, a solution of activity $|AnO_2^{2+}|$ has the same reactivity (for the L^{z_L} ligand) as a solution of activity of $|M^{z_M}| K_{X/VI}^\circ$.

In a third type of analogy, the (b) slope of the linear correlation is no longer 1 ($b \neq 1$), as found here for H^+/M^{z_M} exchanges (b is not correlated with z_M, so it is better not to consider the ($z_M H^+$)/M^{z_M} exchange); $K_1^\circ K_a^\circ$, as its equilibrium constant is no longer a relevant parameter for the analogy: analogue solutions should instead be based on the parameter $10^a = K_1^\circ (K_a^\circ)^b = [(|H^+||L^{z_L}|)^b / (|M^{z_M}||L^{z_L}|)]_{1/2}$, whose interpretation is less intuitive.

Similarly when comparing protonation energies in aqueous and gas phases, the slope of the energy correlation is determined by the ratio of the H^+ activity scales in both phases. It is far from 1 (Fig. 3), corresponding to differences in the orders of magnitude (of the energies of reactions) in each phase. The intercept is related to the balance of the hydration energies (it can be shifted by changing the reference state).

Finally the rules of thumb are often characterized by the value of the (fitted) slopes in linear correlations of equilibrium constants, or equivalently by the value of the corresponding exponent in ratios of activities, the ideal concentrations.

References

[1] V. Phrommavanh, M. Descostes, P. Vitorge, C. Beaucaire, J.-P. Gaudet, Estimating the Stabilities of Aqueous Actinide Complexes with Sulfoxyanions. Poster PA3-9 at the 10th International Conference on Chemistry and Migration Behaviour of Actinides and Fission Products in the Geosphere, MIGRATION'05, September 18–23, 2005. Avignon, France.

[2] I. Grenthe, J. Fuger, R.J.M. Konings, R. Lemire, A.B. Muller, C. Nguyen-Trung, H. Wanner, Chemical Thermodynamics of Uranium download:, Paris OECD/NEA and Elsevier, 1992, http://www.nea.fr/html/dbtdb/pubs/uranium.pdf.

[3] R. Silva, G. Bidoglio, M. Rand, P. Robouch, H. Wanner, I. Puigdomenech, Chemical Thermodynamics of Americium download:, Paris OECD/NEA and Elsevier, 1995, http://www.nea.fr/html/dbtdb/pubs/americium.pdf.

[4] R. Lemire, J. Fuger, H. Nitsche, M. Rand, K. Spahiu, J. Sullivan, W. Ullman, P. Vitorge, Chemical Thermodynamics of Neptunium and Plutonium, Paris OECD/NEA and Elsevier, 2001.

[5] P. Vitorge, H. Capdevila, Radiochim. Acta 91 (2003) 623.

[6] P. Vitorge, H. Capdevila, S. Maillard, M.-H. Fauré, T. Vercouter, J. Nuclear Sci. Technol. 3 (2002) 713.

[7] P. Vitorge, Chimie des actinides. Article and Formulaire form B, Techniques de l'Ingénieur, vol. 3520, 1999.

[8] D. Rai, J.L. Ryan, Inorg. Chem. 24 (1985) 247.

[9] M. Altmaier, V. Neck, T. Fanghänel, Solubility and Ternary Hydroxo-Carbonate Complexes of Thorium, NRC6 2004-03, Sixth International Conference on Nuclear and Radiochemistry, August 29th to September 3rd 2004, Aachen, Germany. http://www.fz-juelich.de/NRC6/.

[10] M. Altmaier, V. Neck, R. Muller, T. Fanghanel, Radiochim. Acta 93 (2) (2005) 83.

[11] E. Gaucher, C. Robelin, J.-M. Matray, G. Negral, Y. Gros, J.-F. Heitz, A. Vinsot, H. Rebours, A. Cassagnabere, A. Bouchet, Phys. Chem. Earth 29 (1) (2004) 55.

[12] C. Beaucaire, P. Toulhoat, Appl. Geochem. 2 (1987) 417.

[13] M. Descostes, C. Beaucaire, F. Mercier, S. Savoye, J. Sow, P. Zuddas, Bull. Soc. Géol. Fr. 173 (2002) 265.

[14] M. Descostes, P. Vitorge, C. Beaucaire, Geochim. Cosmochim. Acta 68 (22) (2004) 4559.

[15] P.L. Brown, E. Curti, B. Grambow, Chemical Thermodynamics of Zirconium, Paris OECD/NEA and Elsevier, 2005.

[16] R. Guillaumont, T. Fanghänel, J. Fuger, I. Grenthe, V. Neck, D.A. Palmer, M.H. Rand, Update on the Chemical Thermodynamics of Uranium, Neptunium, Plutonium, Americium and Technetium, Paris OECD/NEA and Elsevier, 2003.

[17] B. Siboulet, C.J. Marsden, P. Vitorge, Submitted for publication.

[18] R.L. Martin, P.J. Hay, L.R. Pratt, J. Phys. Chem. A 102 (20) (1998) 3565.

[19] G. Choppin, in: J. Rydberg, C. Musikas, G. Choppin (Eds.), Principles and Practices of Solvent Extraction, Marcel Dekker, New York, USA, 1992, p. 71.

[20] B. Allard, J. Rydberg, C. Musikas, G. Choppin, in: J. Rydberg, C. Musikas, G.R. Choppin (Eds.), Principles and Practices of Solvent Extraction, Marcel Dekker, New York, USA, 1992, p. 209.

[21] B. Siboulet, C.J. Marsden, P. Vitorge, Chem. Phys., in press.

[22] A.E. Reed, L.A. Curtiss, F. Weinhold, W. Aas, Chem. Rev. 88 (1988) 899.

[23] E.D. Glendening, A.E. Reed, J.E. Carpenter, F. Weinhold, Natural Population Analysis in Gaussian. NBO Version 3.1, 1998.

[24] M.J. Frisch, G.W. Trucks, H.B. Schlegel, G.E. Scuseria, M.A. Robb, J.R. Cheeseman, V.G. Zakrzewski, J.A. Montgomery Jr., R.E. Stratmann, J.C. Burant, S. Dapprich, J.M. Millam, A.D. Daniels, K.N. Kudin, M.C. Strain, O. Farkas, J. Tomasi, V. Barone, M. Cossi, R. Cammi, B. Mennucci, C. Pomelli, C. Adamo, S. Clifford, J. Ochterski, G.A. Petersson, P.Y. Ayala, Q. Cui, K. Morokuma, D.K. Malick, A.D. Rabuck, K. Raghavachari, J.B. Foresman, J. Cioslowski, J.V. Ortiz, A.G. Baboul, B.B. Stefanov, G. Liu, A. Liashenko, P. Piskorz, I. Komaromi, R. Gomperts, R.L. Martin, D.J. Fox, T. Keith, M.A. Al-Laham, C.Y. Peng, A. Nanayakkara, C. Gonzalez, M. Challacombe, P.M.W. Gill, B.G. Johnson, W. Chen, M.W. Wong, J.L. Andres, M. Head-Gordon, E.S. Replogle, J.A. Pople, Gaussian 98 (Revision A.9), Gaussian, Inc., Pittsburgh PA, 1998.

[25] M.J. Frisch, G.W. Trucks, H.B. Schlegel, G.E. Scuseria, M.A. Robb, J.R. Cheeseman, J.A. Montgomery Jr., T. Vreven, K.N. Kudin, J.C. Burant, J.M. Millam, S.S. Iyengar, J. Tomasi, V. Barone, B. Mennucci, M. Cossi, G. Scalmani, N. Rega, G.A. Petersson, H. Nakatsuji, M. Hada, M. Ehara, K. Toyota, R. Fukuda, J. Hasegawa, M. Ishida, T. Nakajima, Y. Honda, O. Kitao, H. Nakai, M. Klene, X. Li, J.E. Knox, H.P. Hratchian, J.B. Cross, V. Bakken, C. Adamo, J. Jaramillo, R. Gomperts, R.E. Stratmann, O. Yazyev, A.J. Austin, R. Cammi, C. Pomelli, J.W. Ochterski, P.Y. Ayala, K. Morokuma, G.A. Voth, P. Salvador, J.J. Dannenberg, V.G. Zakrzewski, S. Dapprich, A.D. Daniels, M.C. Strain, O. Farkas, D.K. Malick, A.D. Rabuck, K. Raghavachari, J.B. Foresman, J.V. Ortiz, Q. Cui, A.G. Baboul, S. Clifford, J. Cioslowski, B.B. Stefanov, G. Liu, A. Liashenko, P. Piskorz, I. Komaromi, R.L. Martin, D.J. Fox, T. Keith, M.A. Al-Laham, C.Y. Peng, A. Nanayakkara, M. Challacombe, P.M.W. Gill, B. Johnson, W. Chen, M.W. Wong, C. Gonzalez, J.A. Pople, Gaussian 03, Revision C.02, Gaussian, Inc., Wallingford CT, 2004.

[26] P. Robouch, Contribution à la prévision du comportement de l'américium, du plutonium et du neptunium dans la géosphère ; données géochimiques, Thèse n°1987STR13230-SUDOC n° 043589863, Université Louis-Pasteur, Strasbourg, France, 13/11/1987. CEA-R-5473, 1989.

[27] P. Robouch, P. Vitorge, Inorg. Chim. Acta 140 (1/2) (1987) 239.

[28] T. Vercouter, Complexes aqueux de lanthanides (III) et actinides (III) avec les ions carbonate et sulfate. Étude thermodynamique par spectrofluorimétrie laser résolue en temps et spectrométrie de masse à ionisation électrospray. Thèse n°2005EVRY0003-SUDOC n° 09483699X, Université d'Évry, France, 2005.

[29] P. Vitorge, H. Capdevila, CEA-R-5793, 1998.

[30] E. Osthols, J. Bruno, I. Grenthe, Geochim. Cosmochim. Acta 58 (2) (1994) 613.

[31] N. Eglizaud, M. Descostes, M. Schlegel, E. Simoni, 10es Journées nationales de radiochimie et de chimie nucléaire, Avignon, France, 7−8/09/2006.

[32] N. Eglizaud, F. Miserque, E. Simoni, M. Schlegel, M. Descostes, MIGRATION'05, Avignon, France, 18−23/09/2005.

[33] C. Jaussaud, Contribution à l'étude thermodynamique de l'hydrolyse de Pa(V) à l'échelle des traces par la technique d'extraction liquide−liquide avec la TTA, Thèse, Université Paris-Sud, Orsay, 2003.

[34] D. Trubert, C. Le Naour, C. Jaussaud, J. Solution Chem. 31 (4) (2002) 261.

[35] D. Trubert, C. Le Naour, C. Jaussaud, O. Mrad, J. Solution Chem. 32 (6) (2003) 505.

[36] C. Peiffert, Solubilité et hydrolyse du niobium en solution aqueuse à 25 °C et 0.1 Mpa, Poster, Journées scientifiques ANDRA, Nancy (France), 7−9 décembre 1999.